(45) Strazielle, C. *Eur. Polym. J.* **1979**, *15*, 55.
(46) Kratochvíl, P.; Vorlíček, J. *J. Polym. Sci., Polym. Phys. Ed.* **1976**, *14*, 1561.
(47) Kratochvíl, P.; Vorlíček, J.; Strakova, D.; Tuzar, Z. *J. Polym. Sci., Polym. Phys. Ed.* **1975**, *13*, 2321.
(48) Kratochvíl, P.; Straková, D.; Tuzar, Z. *Br. Polym. J.* **1977**, *9*, 217.
(49) Kratochvíl, P.; Straková, D.; Podešva, J. *J. Polym. Sci., Polym. Phys. Ed.* **1979**, *17*, 945.
(50) Campos, A.; Strazielle, C. *Eur. Polym. J.* **1978**, *14*, 517.
(51) Heitz, W.; Kern, W. *Angew. Makromol. Chem.* **1967**, *1*, 150.
(52) Sitaramaiah, G.; Jacobs, D. *Polymer*, **1970**, *11*, 165.
(53) Ouano, A. C.; Gipstein, E.; Kaye, W.; Dawson, B. *Macromolecules* **1975**, *8*, 558.
(54) Cazes, J.; Gaskill, D. R. *Sep. Sci.* **1969**, *4*, 15.
(55) Cazes, J.; Gaskill, D. R. *Sep. Sci.* **1967**, *2*, 421.
(56) Cazes, J.; Herron, S. *Sep. Sci.* **1973**, *8*, 395.
(57) Horta, A. *J. Macromol. Sci., Chem.* **1971**, *5*, 487.

Conformational Characteristics of Poly(2-vinylpyridine)

A. E. Tonelli

AT&T Bell Laboratories, Murray Hill, New Jersey 07974. *Received May 10, 1985*

ABSTRACT: Conformational energy calculations were coupled with dipole moment measurements to derive a conformational description of poly(2-vinylpyridine) (P2VP). When a rotational isomeric states (RIS) model was used to calculate the dipole moments of P2VP chains with different stereosequences, it was found that the calculated dipole moments were nearly independent of P2VP stereosequence. Dipole moments measured for three P2VP samples with very different stereosequences, as determined by ^{13}C NMR spectroscopy, were also very similar with magnitudes that agreed with the calculated dipole moments. In addition, the isomer fractions observed by Hogen-Esch et al. after the equilibrium epimerization of P2VP oligomers are also successfully reproduced by the RIS model developed here for P2VP.

Introduction

It has been observed[1-8] that vinyl polymers possessing large, planar side groups are limited in their conformational freedom. Previous studies of such vinyl polymers, i.e., poly(methyl methacrylate),[1,2] poly(methyl acrylate),[3] poly(vinyl acetate),[4] polystyrene,[5] poly(α-methylstyrene),[6] poly(*N*-vinylcarbazole),[7] and poly(*N*-vinylpyrrolidone),[8] led to the observation that the planarity of the side groups severely limits the conformations (ϕ_1,ϕ_2) available to the pair of backbone bonds flanked by these large, rigid side groups (see Figure 1). Poly(2-vinylpyridine) (P2VP) is another example of a vinyl polymer with planar side groups.

The pyridine side groups in P2VP are polar (see Figure 1) and may interact with each other in certain backbone conformations, such as the tt conformation of the meso (m) P2VP diad illustrated in Figure 1. In this conformation access of the backbone to solvent molecules is limited, a situation that also arises in the tg^- conformation of a racemic (r) P2VP diad. Thus, we might expect the conformations adopted by the P2VP backbone to depend not only on stereosequence but also on solvent interactions and side-group orientations.

We have studied the conformational characteristics of P2VP chains by employing approximate potential energy functions to estimate their conformational energies. In addition to treating P2VP chains of different stereoregularity, side groups were permitted to adopt different orientations and solvent interaction energies were approximated. A rotational isomeric states (RIS) model was derived for P2VP from the conformational energy estimates. Mean-square unperturbed dimensions (end-to-end chain lengths) and dipole moments were calculated as a function of stereoregularity from the RIS model derived here for P2VP and were compared to dilute solution dimensions reported in the literature and to the dipole moments measured in the present study for three P2VP samples with different stereosequences.

Conformational Energies

Method of Calculation. The recently reported[9] crystal structure of 2,4,6,8-tetramethyl-2,4,6,8-tetra-2-pyridylnonane provides us with geometric information concerning the side groups in P2VP. The pyridine rings are planar and are very similar to phenyl rings in their geometry. As an example, the pyridine ring bond lengths and valence angles span the ranges 1.34–1.41 Å and 117–124°, while 1.39 Å and 120° are found[10] for phenyl rings. Consequently, we have used the geometrical parameters employed by Yoon et al.[5] in their treatment of polystyrene to calculate the conformational energies of P2VP.

Rotation about each backbone C–C bond was assigned a threefold intrinsic torsional potential with a barrier height of 2.8 kcal/mol. A Lennard-Jones 6–12 potential together with a Coulombic term were used to evaluate the nonbonded van der Waals and electrostic interactions between atoms. Parameters of the 6–12 potential were the same as those employed by Yoon et al.[5] for polystyrene and by us[8] for poly(*N*-vinylpyrrolidone). From the dipole moment measured[11] for pyridine in dilute solutions (2.25 D), partial charges of −0.68 and +0.34 were assigned respectively to the N atom and the two C atoms bonded to it, and a dielectric constant of 3.5 was assumed to mediate the electrostatic interactions.

Certain conformations of vinyl polymers with large side-chain substituents can prevent solvent molecules from gaining access to the polymer backbone (see Figure 1). However, for an m diad in the tg^- conformation the side chains are sufficiently separated to permit access of the solvent. By replacing side-chain–side-chain interactions with side-chain–solvent interactions when the the distance r between side chains becomes sufficiently great ($r = \sigma$), Yoon et al.[5] devised a procedure to account for the conformational dependence of solvent interactions. The energy of interaction should level off at the distance σ, and we therefore require the calculated conformational energy to remain constant at its value for $r = \sigma$ for all distances greater than σ. Judging from previous results[1-8] σ = 4–5 Å seems reasonable, and we have employed σ = 4.5 Å and ∞ (no solvent–polymer interactions considered) in our calculations on P2VP.

Backbone rotation angles ϕ_1 and ϕ_2 were stepped in 10° increments and were measured in a right-handed sense (a different rotation angle sign convention was employed in

0024-9297/85/2218-2579$01.50/0

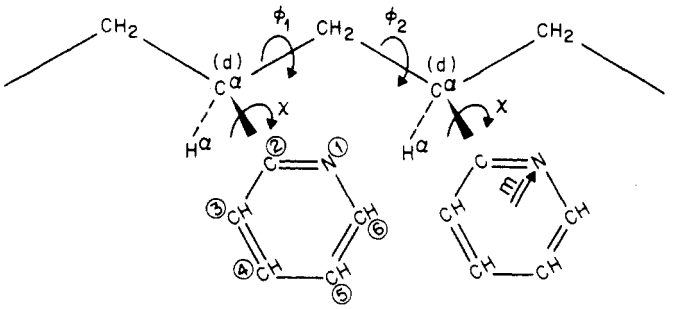

Figure 1. A meso or m (d,d) diad in the tt conformation ($\phi_1 = \phi_2 = 0°$) along the P2VP chain. The location of the pyridine side group dipole moment is noted by m.

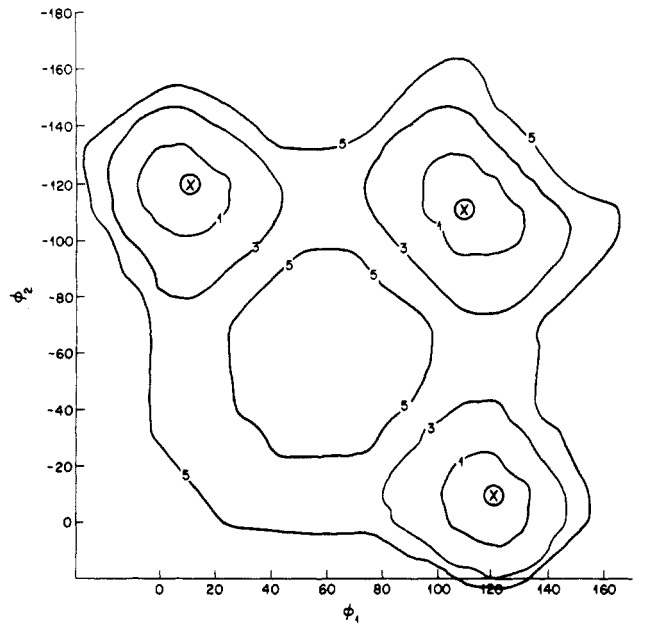

Figure 2. Conformational energy map for a meso (d,d) PVP diad calculated with $\chi = 180°$ and $\sigma = 4.5$ Å. × indicates the locations of the lowest energy conformations at $\phi_1, \phi_2 = 10°, -120°; 120°, -10°$; and 110°, -110°. The contours are drawn in units of kcal mol^{-1} relative to ×.

ref 1–7). Two orientations (x) of the pyridine ring were permitted: $x = 0°$, where C_2–N and C^α–H^α are eclipsed, and $x = 180°$, where C_2–C_3 and C^α–H^α are eclipsed (see Figure 1). Both allowed side-chain orientations have the plane of the pyridine ring bisecting the valence angle ($\angle CH_2$–$C^\alpha H$–CH_2) defined by the backbone bonds flanking the C^α carbon to which it is attached. Previous studies[12,13] have indicated that only small deviations (10–30°) from $x = 0$ or 180° are permitted by the resultant steric interactions.

Results. Conformational energy maps for meso (d,d) and racemic (d,l) P2VP diads are presented in Figures 2 and 3. Both conformational energy maps make apparent that backbone conformations that result in the simultaneous gauche arrangements of C^α, CH_2, and the pyridine side chain (Pyr), such as

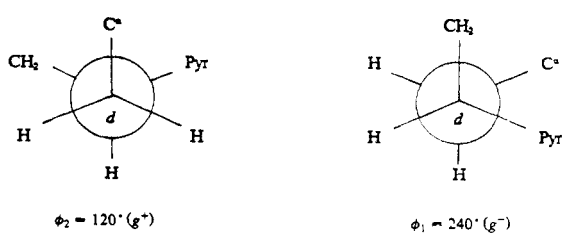

are precluded. Each of the backbone bonds in P2VP is

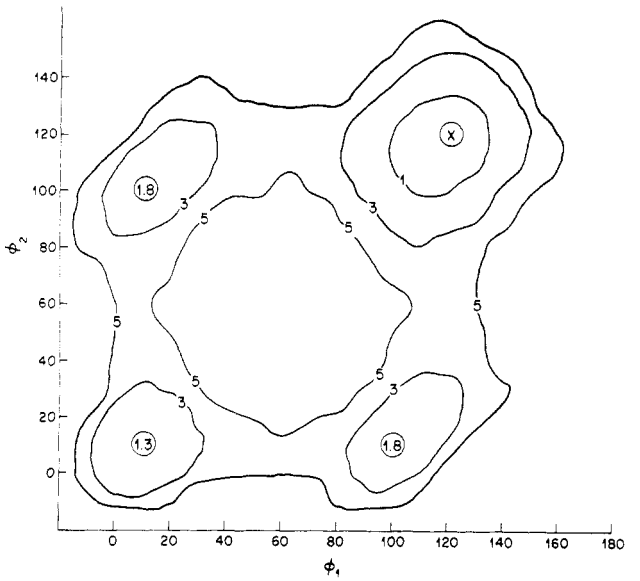

Figure 3. Same as Figure 2 except replace meso (d,d) with racemic (d,l) and $\phi_1, \phi_2 = 10°, -120°; 120°, -10°$; and 110°, -110° with $\phi_1, \phi_2 = 120°, 120°$.

Table I
Partition Functions (Z_s), Average Energies ($\langle E_s \rangle$), and Preexponential Factors (α_s) for the Various Low-Energy P2VP Diad Conformations As Obtained from Their Energy Maps

	Z_s[a]		$\langle E_s \rangle$, kcal/mol		α_s	
state (s)	σ = 4.5 Å	$\sigma = \infty$	σ = 4.5 Å	$\sigma = \infty$	σ = 4.5 Å	$\sigma = \infty$
d,d; tt	0.10	0.41	1.45	0.49	0.99	0.87
d,d; tg^-	2.79	1.0	−0.73	0.03	0.90	0.96
d,d; g^+t	2.79	1.0	−0.73	0.03	0.90	0.96
d,d; g^+g^-	3.77	0.58	−0.68	0.56	1.31	1.38
d,l; tt	1.0	1.0	0.0	0.0	1.0	1.0
d,l; tg^+	0.44	0.11	0.76	1.78	1.44	1.74
d,l; g^+t	0.44	0.11	0.76	1.78	1.44	1.74
d,l; g^+g^+	7.29	1.37	−0.98	0.09	1.59	1.58

[a] $Z_s = \alpha_s \exp[-\langle E_s \rangle / RT]$, T = 50 °C.

thus limited to just two rotational states. Similar rotational restrictions were observed[1-8] in the conformational studies of other vinyl polymers with bulky side groups.

Though the value of σ used to approximate the solvent–polymer interactions influenced the relative energies of the allowed backbone conformations, restriction of each backbone bond to just two rotational states was found to be independent of σ. We therefore limit our consideration to just two rotational states for each backbone bond, which leads to 2 × 2 statistical weight matrices, in our derivation of an RIS model for P2VP.

P2VP RIS Model

For the bond pairs flanking and between substituted C^α carbons we may write[5] statistical weight matrices U′ and U″

$$U' = \begin{bmatrix} 1 & 1 \\ 1 & 0 \end{bmatrix} \qquad U'' = \begin{bmatrix} Z_{tt} & Z_{tg^\pm} \\ Z_{g^\pm t} & Z_{g^\pm g^\pm} \text{ or } Z_{g^\pm g^\mp} \end{bmatrix} \quad (1)$$

Z_s are the partition functions of the low-energy-conformation domains and may be evaluated from the energy maps according to $Z_s = \alpha_s \exp[-\langle E_s \rangle / RT]$, where α_s and $\langle E_s \rangle$ are the preexponential factor (breadth) and average energy (depth) of each conformational domain s. Table I presents such an evaluation for the d,d-meso and d,l-racemic P2VP diads from Figures 2 and 3, where the racemic tt domain is assigned a zero average energy.

The statistical weight matrices can also be expressed[5,14] in terms of the first- and second-order interaction parameters[15] dependent upon a single or a pair of rotations

$$U'_d = \begin{matrix} t \\ g^- \end{matrix}\begin{bmatrix} t & g^+ \\ 1 & 1 \\ 1 & 0 \end{bmatrix} \qquad U'_l = \begin{matrix} t \\ g^+ \end{matrix}\begin{bmatrix} t & g^- \\ 1 & 1 \\ 1 & 0 \end{bmatrix} \tag{2}$$

$$U''_{d,d} = \begin{matrix} t \\ g^+ \end{matrix}\begin{bmatrix} t & g^- \\ \omega'' & 1/\eta \\ 1/\eta & \omega/\eta^2 \end{bmatrix} \qquad U''_{l,l} = \begin{matrix} t \\ g^- \end{matrix}\begin{bmatrix} t & g^+ \\ \omega'' & 1/\eta \\ 1/\eta & \omega/\eta^2 \end{bmatrix} \tag{3}$$

$$U''_{d,l} = \begin{matrix} t \\ g^+ \end{matrix}\begin{bmatrix} t & g^+ \\ 1 & \omega'/\eta \\ \omega'/\eta & 1/\eta^2 \end{bmatrix} \qquad U''_{l,d} = \begin{matrix} t \\ g^- \end{matrix}\begin{bmatrix} t & g^- \\ 1 & \omega'/\eta \\ \omega'/\eta & 1/\eta^2 \end{bmatrix} \tag{4}$$

where the racemic (d,l; l,d) tt state is given a statistical weight of unity. From the results of the conformational energy calculations, as summarized in Table I, we obtain the following solutions for the first- and second-order interaction parameters: $\omega = 1.4 \exp(-340/T)$, $\omega' = 1.6 \exp(-820/T)$, $\omega'' = 0.9 \exp(-E_{\omega''}/RT)$, where $E_{\omega''} = 0.5$–1.5 kcal/mol, and $\eta = 1.0 \exp(-E_\eta/RT)$, where $E_\eta = -0.1$ to $+0.8$ kcal/mol. η and ω'' describe the first- and second-order interactions[15] involving the pyridine side groups and consequently are sensitive to σ. This results in a range of possible values for E_η and $E_{\omega''}$. E_ω and $E_{\omega'}$ are not sensitive to ω because they characterize the second-order interactions[15] between CH_2, CH_2 and CH_2, Pyr, which do not involve the close approach of two neighboring Pyr rings.

Dipole Moments and Dimensions

Measurement of P2VP Dipole Moments. A WTW Dipolmeter using a DFL-1 dielectric cell with thermostatic control was used to measure the dielectric constants of P2VP solutions. Solution refractive indices were obtained with a Bausch and Lomb Abbe-type refractometer.

Three samples of P2VP with different stereosequences were studied: two commercial samples of atactic P2VP with molecular weights of 20000 and a sample of isotactic P2VP with a molecular weight of 45000. High-resolution solution ^{13}C NMR spectra were recorded for each sample, and analysis[16-18] of the C_2 carbon (see Figure 1) region revealed the following stereosequence information: (i) one of the atactic P2VP samples (A-1) is Bernoullian with $P_m = 0.5$, i.e., a random distribution of m and r diads, (ii) the other atactic P2VP (A-2) is non-Bernoullian and is characterized by $P_{mm} = 0.44$, $P_{mr} = P_{rm} = 0.18$, and $P_{rr} = 0.20$, and (iii) the isotactic P2VP (I) has $P_{mm} \sim 0.9$.

The dipole moments of the atactic samples were measured in benzene at 25 °C, while it was necessary to initially dissolve the isotactic P2VP (I) in refluxing *p*-dichlorobenzene and subsequently perform the dielectric measurements at 80 °C in this solvent. Solutions of weight fractions $W_2 = 0.5$–2% were employed. The measured dielectric constant ϵ and refractive index n depended linearly on W_2 and were fitted to the following equations:

$$\epsilon = \epsilon_1(1 + \alpha W_2) \tag{5}$$

$$n = n_1(1 + \gamma W_2) \tag{6}$$

where 1 and 2 denote solvent and solute, respectively.

The Smith and Guggenheim[19] equation

$$\langle \mu^2 \rangle = \frac{27kTM}{4\pi N_A d_1(\epsilon_1 + 2)^2}(\alpha\epsilon_1 - 2n_1^2\gamma) \tag{7}$$

was used to obtain mean-square dipole moments $\langle \mu^2 \rangle$, where M is the molecular weight of P2VP solute, $d_1 = 0.8786$ and 1.2475, $\epsilon = 2.274$ and 2.356, and $n_1 = 1.49816$ and 1.5285 are densities, dielectric constants, and refractive indices of benzene at 25 °C and *p*-dichlorobenzene at 80 °C, and N_A is Avogadro's number. The observed $\langle \mu^2 \rangle$ are presented in Table II.

Table II
Dipole Moments ($\langle \mu^2 \rangle / x$) Measured for P2VP

sample	stereoregularity	$\langle \mu^2 \rangle / x$, D^2
A-1	atactic, Bernoullian P2VP with $P_m = 0.5$	3.1[a]
A-2	atactic, non-Bernoullian P2VP with $P_{mm} = 0.44$, $P_{mr} = P_{rm} = 0.18$, and $P_{rr} = 0.20$	2.8[a]
I	isotactic with $P_{mm} \sim 0.9$	3.3[b]

[a] Measured in benzene at 25 °C. [b] Estimated by comparing the Dipolmeter readings obtained for 1.7 wt % solutions of samples I and A-2 in 1,4-dichlorobenzene at 80 °C.

P2VP Dimensions from the Literature. Arichi[20] and Dondos[21] have reported the unperturbed dimensions of atactic P2VP as determined by intrinsic viscosity–molecular weight studies. Conversion of their results to characteristic ratios $C_r = \langle r^2 \rangle_0 / nl^2$, where $\langle r^2 \rangle_0$ is the unperturbed mean-square end-to-end distance and n is the number of backbone bonds of length l in the chain, leads to $C_r = 7$–10 depending on solvent and temperature. Arichi[20] studied fractionated, free radical polymerized samples of P2VP, while Dondos[21] used fractions of an anionically polymerized sample. Based on ^{13}C NMR studies[16-18] of similarly polymerized samples of P2VP, Arichi's polymers were probably atactic and Bernoullian with $P_m \sim 0.5$ and the anionic materials non-Bernoullian with $P_{mm} > 0.25$.

Calculated Dipole Moments and Dimensions

Mean-square dipole moments $\langle \mu^2 \rangle_0$ and dimensions $\langle r^2 \rangle_0$ of 400-bond P2VP chains were calculated by matrix multiplication techniques.[15] The chains were Monte Carlo generated a repeat unit at a time, allowing the entire range of stereosequence to be considered. Bernoullian P2VP chains with $P_m = 0.0$–1.0 and non-Bernoullian chains with $P_{mm} = 0.44$, $P_{mr} = P_{rm} = 0.18$, and $P_{rr} = 0.20$ were generated to mimic the stereosequences found for the three P2VP samples examined in this study. The backbone rotational states t and $g^\pm$ were assigned 0 and $\pm 120°$, and the calculations were performed at 0, 50, and 100 °C.

The dipole moment (2.25 D) measured for pyridine[11] was located as indicated in Figure 1 and was transformed from the pyridine side group to the usual coordinate system[15] along the C^α–CH_2 backbone bond to the right of the C^α carbon to which the ring is attached. To achieve this dipole moment transformation we must specify the orientation x of the pyridine ring with respect to the backbone. We found the probabilities for the $x = 0°$ and $x = 180°$ orientations to be 0.77 (0.71) and 0.23 (0.29) at 0 °C (100 °C), with only a minor dependence on stereosequence. This results in

$$m = \begin{bmatrix} 0.794 \\ -1.179 \\ \pm 0.374d,l \end{bmatrix} D \text{ (50 °C)} \tag{8}$$

expressed in the reference frame along the C^α–CH_2 backbone bond.

The ratios $C_m = \langle \mu^2 \rangle_0 / x$, where x is the number of repeat units, and $C_r = \langle r^2 \rangle_0 / nl^2$ calculated at 0 and 50 °C for $E_{\omega''} = 0.9$ kcal/mol and $E_\eta = -0.1$ kcal/mol are presented in Table III. Both ratios are calculated for Bernoullian P2VP chains with stereosequences ranging from syndiotactic ($P_m = 0.0$) to isotactic ($P_m = 1.0$). Using the same energy parameters ($E_{\omega''}$ and E_η) to calculate the dipole moments and dimensions of a non-Bernoullian P2VP with $P_{mm} = 0.44$, $P_{mr} = P_{rm} = 0.18$, and $P_{rr} = 0.20$ yields $C_m = 2.76$ D^2 and $C_r = 7.2$ at 25 °C. These are nearly identical with the values obtained at $P_m \sim 0.5$ for the Bernoullian, atactic P2VP chains shown in Table III. It is clear from Table

Table III
$C_m = \langle\mu^2\rangle_0/x$ and $C_r = \langle r^2\rangle_0/nl^2$ Calculated for 400-Bond P2VP Chains with Bernoullian Probability P_m for Meso (m) Diad Addition[a]

	C_m		C_r	
P_m	0 °C	50 °C	0 °C	50 °C
0.0	3.06	2.93	11.2	11.1
0.1	3.10	2.98	9.74	9.66
0.2	3.07	2.96	8.50	8.43
0.3	2.99	2.97	7.82	7.72
0.4	2.93	2.85	7.39	7.27
0.5	2.89	2.77	7.18	7.01
0.6	2.77	2.72	7.18	6.95
0.7	2.74	2.70	7.39	7.07
0.8	2.74	2.68	7.65	7.23
0.9	2.82	2.73	8.29	7.68
1.0	2.97	2.83	9.08	8.23

[a] $E_{\omega''} = 0.9$ kcal/mol and $E_\eta = -0.1$ kcal/mol. For $P_m = 0.1$–0.9 10 Monte Carlo chains were generated and C_m and C_r were averaged over this ensemble.

III that the calculated dipole moments of P2VP chains are nearly independent of their stereosequence. In addition the C_m's calculated with $E_{\omega''} = 0.9$ kcal/mol and $E_\eta = -0.1$ kcal/mol agree closely with those measured (see Table II) for three samples of P2VP with different stereosequences.

The insensitivity of the dipole moments of P2VP chains to their stereosequence is in marked contrast to two other vinyl polymers with polar/planar ring side chains. Poly(*p*-chlorostyrene) (PPCS)[22] and poly(*N*-vinylpyrrolidone) (PVP)[8] both exhibit calculated dipole moments that depend significantly on chain stereosequence. Isotactic PPCS and PVP chains have predicted C_m's 1.5 and 3–5 times larger than the dipole moments calculated for their syndiotactic and atactic chains, while for P2VP $C_m = 2.9 \pm 0.2$ D^2 over the complete range of stereoregularity. Apparently the orientation (with respect to the backbone) of the dipole moment in the side chain and differences in the RIS descriptions of these vinyl polymers result in rather dramatic changes in the dependence of their dipole moments on stereosequence.

The dimensions calculated from the RIS model developed here for P2VP chains with atactic stereosequences are $C_r = 7$–8 irrespective of their Bernoullian or non-Bernoullian natures, and they fall in the experimentally observed[20,21] range of $C_r = 7$–10. In the range of stereosequences characterized by $P_m = 0.2$–0.8, the calculated dimensions, like the dipole moments, are insensitive to P2VP stereosequence. Only the C_r's for highly syndiotactic ($P_m = 0.0$–0.1) and highly isotactic ($P_m = 0.9$–1.0) P2VP chains show modest predicted increases over those expected and observed for actactic P2VP.

The calculated dipole moments and dimensions both decrease with increasing temperature. For atactic P2VP $d \ln \langle\mu^2\rangle_0/dT = -0.5 \times 10^{-3}$ °C^{-1} and $d \ln \langle r^2\rangle_0/dT = -0.5$ to -1.0×10^{-3} °C^{-1}. Dondos[21] found the unperturbed dimensions of P2VP to decrease between 15 and 40 °C and then increase between 40 and 60 °C when dissolved in benzene or tetrahydrofuran. In ethanol and chloroform Dondos observed the unperturbed dimensions of P2VP to be independent of temperature and to be 10–15% larger than those measured in benzene and tetrahydrofuran. This unusual dependence of C_r upon temperature and solvent was attributed to the effects of both inter- and intramolecular hydrogen bonding.

Discussion

We have developed a RIS model describing the conformational characteristics of P2VP. This RIS model may be summarized by the following set of statistical weights that account for the relative strengths of the first- and second-order intrachain interactions occurring in P2VP: $\omega = 1.4 \exp(-340/T)$, $\omega' = 1.6 \exp(-820/T)$, $\omega'' = 0.9 \exp(-450/T)$, and $\eta = 1.0 \exp(50/T)$. Steric interactions between the planar pyridine side groups restrict each backbone bond to just two rotational states. Each of the pyridine rings can assume two different orientations with respect to the backbone characterized by $x = 0$ and 180° (see Figure 1), with the former orientation favored by a factor of 2.5–3.

This RIS model successfully predicts the dimensions and dipole moments observed for P2VP, including the independence of the latter property to P2VP chain stereosequence.

As an additional means to test the validity of our RIS model for P2VP, we may compare isomer fractions measured for P2VP oligomers after equilibrium epimerization by Hogen-Esch et al.[23,24] to those calculated[25,26] from the P2VP RIS model. Such a comparison is presented in Table IV for the dimer, trimer, and tetramer oligomers of P2VP, and excellent agreement is observed between the calculated and observed equilibrium isomer fractions.

Table IV
Isomer Fraction f for the Dimer, Trimer, and Tetramer Oligomers of P2VP

	f	
oligomer (isomer)	calcd[a]	obsd[b]
dimer (m)	0.52	0.49
dimer (r)	0.48	0.51
trimer (mm)	0.24	0.23
trimer (mr + rm)	0.51	0.50
trimer (rr)	0.25	0.27
tetramer (mmm)	0.10	0.09
tetramer (mmr + rmm)	0.25	0.25
tetramer (mrm)	0.14	0.13
tetramer (rrm + mrr)	0.26	0.25
tetramer (rmr)	0.13	0.14
tetramer (rrr)	0.12	0.14

[a] At $T = 25$ °C. [b] Measured[29] by gas chromatography after epimerization at 25 °C in *t*-BuOK/Me_2SO for 150–300 h.

Acknowledgment. I am indebted to F. C. Schilling for recording ^{13}C NMR spectra, to Prof. T. E. Hogen-Esch for providing two characterized samples of P2VP, to M. Y. Hellman for intrinsic viscosity measurements, and to Andrew E. Tonell for assistance in the dipole moment measurements.

Registry No. P2VP (homopolymer), 25014-15-7; isotactic-P2VP (homopolymer), 25585-16-4.

References and Notes

(1) Sundararajan, P. R.; Flory, P. J. *J. Am. Chem. Soc.* **1974**, *96*, 5025.
(2) Sundararajan, P. R. *J. Polym. Sci., Polym. Lett. Ed.* **1977**, *15*, 699.
(3) Yoon, D. Y.; Suter, U. W.; Sundararajan, P. R.; Flory, P. J. *Macromolecules* **1975**, *8*, 284.
(4) Sundararajan, P. R. *Macromolecules* **1978**, *11*, 256.
(5) Yoon, D. Y.; Sundararajan, P. R.; Flory, P. J. *Macromolecules* **1975**, *8*, 776.
(6) Sundararajan, P. R. *Macromolecules* **1977**, *10*, 623.
(7) Sundararajan, P. R. *Macromolecules* **1980**, *13*, 512.
(8) Tonelli, A. E. *Polymer* **1982**, *23*, 676.
(9) Avenel, P. D.; Ades, D.; Smith, R. A.; Hogen-Esch, T. E. *Acta. Crystallogr., Sect. B: Struct. Crystallogr. Cryst. Chem.* **1982**, *B38*, 1611.
(10) Wyckoff, R. W. G. "Crystal Structures; 2nd ed.; Interscience: New York, 1969; Vol. 6.
(11) McClellan, A. L. "Tables of Experimental Dipole Moments", W. H. Freeman: San Francisco, 1963.
(12) Abe, Y.; Tonelli, A. E.; Flory, P. J. *Macromolecules* **1970**, *3*, 294.
(13) Tonelli, A. E. *Macromolecules* **1973**, *6*, 682.

(14) Suter, U. W.; Flory, P. J. *Macromolecules* **1975**, *8*, 765.
(15) Flory, P. J. "Statistical Mechanics of Chain Molecules"; Wiley-Interscience: New York, 1969; Chapters I–VI.
(16) Brigidiot, M.; Cheradame, H.; Fontanille, M.; Vairon, J. P. *Polymer* **1976**, *17*, 254.
(17) Matsuzaki, K.; Kanai, T.; Matsubara, T.; Matsumoto, S. *J. Polym. Sci., Polym. Chem. Ed* **1976**, *14*, 1475.
(18) Matsuzaki, K.; Matsubara, T.; Kanai, T. *J. Polym. Sci., Polym. Chem. Ed.* **1977**, *15*, 1573.
(19) Bottcher, C. T. F.; Bordewijk, P. "Theory of Dielectric Polymerization"; Elsevier: Amsterdam, 1978; Vol. II, Chapter 14.
(20) Arichi, S. *Bull. Chem. Soc. Jpn.* **1966**, *39*, 439.
(21) Dondos, A. *Makromol. Chem.* **1970**, *135*, 181.
(22) Saiz, E.; Mark, J. E.; Flory, P. J. *Macromolecules* **1977**, *10*, 967.
(23) Hogen-Esch, T. E.; Tien, C. F. *Macromolecules* **1980**, *13*, 207.
(24) Hwang, S. S.; Mathis, C.; Hogen-Esch, T. E. *Macromolecules* **1981**, *14*, 1802.
(25) Flory, P. J. *J. Am. Chem. Soc.* **1967**, *89*, 1798.
(26) Suter, U. W. *Macromolecules* **1981**, *14*, 523.

Analysis of the Crystalline Phase Transformation of Poly(vinylidene fluoride)

S. L. Hsu,* F. J. Lu, D. A. Waldman, and M. Muthukumar

Polymer Science and Engineering Department, University of Massachusetts, Amherst, Massachusetts 01003. *Received September 28, 1984*

ABSTRACT: Infrared spectra have been obtained at various temperatures for poly(vinylidene fluoride) in the presence of electric fields up to 5.2 MV/cm in strength. Quantitative analysis of the spectroscopic data suggests that significant $\alpha \rightarrow \beta$ or $\alpha \rightarrow \gamma$ phase transformations can occur at electric fields as low as 1.2 MV/cm. The kinetics of these transformations have been studied. Our data show the degree of phase transformation also depends strongly on the temperature.

Introduction

Poly(vinylidene fluoride) (PVF_2) is the most widely known polymer that exhibits piezoelectric or pyroelectric properties. At least four crystalline phases, α, β, γ, and δ, have been found for PVF_2, with one or two more under study.[1] It is now generally accepted that the existence or absence of a net polarization determines whether the crystalline phase is electrically active.[2,3] The β phase, with a nearly planar zigzag conformation, has the highest piezoelectric constant.[1,4] Although the α phase, with a TGTG′ conformation, is electrically inactive, the δ phase, which is nearly identical with the α phase except that every other chain is effectively rotated, is electrically active.[3] The obvious connection between the crystalline structure and the resultant electrical property has led to many attempts to prepare different phases by various methods that include altering the thermal history,[5] mechanical deformation,[6] γ radiation,[7] crystallization under high pressure,[8] crystallization under electric field,[9] and the application of a strong electric field.[10–12] The last method is fundamentally interesting because exact mechanisms have not yet been determined and is practically important because it is effective in the enhancement of PVF_2's electrical properties.

The electrical-field-induced microstructural changes in PVF_2 may depend on field strength, temperature, and/or time. The transition that has received the most attention is probably the $\alpha \rightarrow \delta$ or $\alpha \rightarrow \beta$ transition. The initial report on the possibility of an $\alpha \rightarrow \beta$ transition is by Luongo for a field of 0.3 MV/cm.[13] The field strength is considerably weaker than those determined in later studies.[10–12] Davis and co-workers eventually concluded that the $\alpha \rightarrow \delta$ transition can occur at low field strengths ($\sim$1.5 MV/cm) while the subsequent transition to the β phase can only occur at high field strengths of 4–5 MV/cm.[11] Several theoretical studies followed these experimental studies to consider the relative stability of each crystalline phase, their coupling to the applied field, the dynamics of structural change, and the critical field values.[14,15] However, the predictions of those theories have not been tested because of the difficulties involved in obtaining direct experimental evidence to characterize microstructural changes in the presence of an electric field.

In our laboratory we are using vibrational spectroscopy as the primary characterization technique. In the infrared spectra of PVF_2 there are absorptions that are characteristic of local conformations or environments that can be used to monitor microstructural changes induced by external electrical excitation.[16–23]. Using an experimental geometry suggested earlier,[18] we have used Fourier transform infrared spectroscopy to directly measure the electric field molecular motions of various phases of PVF_2 with high sensitivity, wide spectral response, and high time resolution.[19,20] In the present study we have carried out additional experiments as a function of field strength, temperature, and time and obtained a quantitative assessment of the relative fractions of different crystalline phases present. We found that the $\alpha \rightarrow \delta$ or $\alpha \rightarrow \beta$ phase transformation can take place at a much faster rate and lower field strength than previously reported theoretical or experimental values.[10–12,14,15]

Although a number of theoretical studies are under way,[19,20] details of the exact molecular mechanism associated with phase transformations in PVF_2 are still ill-understood; incorporation of experimental results such as the ones reported here is both interesting and relevant.

Experimental Section

The 6-, 12-, and 24-μm-thick PVF_2 films used in our studies were obtained from Kureha Chemical Corp. Details of the experimental geometry used can be found in previous publications.[21,22] Gold–palladium electrodes 1.2 cm in diameter were deposited on both sides of the film. The deposited electrodes are sufficiently thick to conduct electricity, yet thin enough to transmit infrared radiation. We used a high-voltage power supply capable of providing 3000 V or the equivalent to a maximum field strength of 5 MV/cm for the 6-μm-thick samples. The entire sample was placed in a heating cell so that experiments could be carried out at temperatures between ambient and 150 °C in an inert atmosphere.

Infrared spectra were obtained with a Nicolet Fourier transform infrared spectrometer. Since we are mainly interested in the

0024-9297/85/2218-2583$01.50/0